ADVANCED MATERIALS
www.advmat.de

Flexible Temperature-Invariant Polymer Dielectrics with Large Bandgap

Chao Wu, Ajinkya A. Deshmukh, Zongze Li, Lihua Chen, Abdullah Alamri, Yifei Wang, Rampi Ramprasad, Gregory A. Sotzing, and Yang Cao**

Flexible dielectrics operable under simultaneous electric and thermal extremes are critical to advanced electronics for ultrahigh densities and/or harsh conditions. However, conventional high-performance polymer dielectrics generally have conjugated aromatic backbones, leading to limited bandgaps and hence high conduction loss and poor energy densities, especially at elevated temperatures. A polyoxafluoronorbornene is reported, which has a key design feature in that it is a polyolefin consisting of repeating units of fairly rigid fused bicyclic structures and alkenes separated by freely rotating single bonds, endowing it with a large bandgap of ≈5 eV and flexibility, while being temperature-invariantly stable over −160 to 160 °C. At 150 °C, the polyoxafluoronorbornene exhibits an electrical conductivity two orders of magnitude lower than the best commercial high-temperature polymers, and features an unprecedented discharged energy density of 5.7 J cm^{-3} far outperforming the best reported flexible dielectrics. The design strategy uncovered in this work reveals a hitherto unexplored space for the design of scalable and efficient polymer dielectrics for electrical power and electronic systems under concurrent harsh electrical and thermal conditions.

Rapid growth of renewable offshore wind energy, electrification in land, sea, and air transportations, downhole oil and gas drilling and lifting, outer space explorations, all call for flexible dielectrics with ultrahigh energy and power densities.[1–7] With the maturing of wide bandgap semiconductors (e.g., SiC, GaN), the electrical and electronic systems could be designed with unprecedentedly high power density and payload efficiency[8–10] if new flexible dielectric materials could be made available to operate concurrently under high electric fields and elevated temperatures approaching or surpassing 150 °C.[2,4,8,11–13] However, to date, the search for polymer dielectrics that provide appreciable energy densities at temperatures well above 100 °C has led to only marginal success. High temperature operation under high electric field is challenging for polymer dielectrics. For example, biaxially oriented polypropylene (BOPP), the state-of-the-art commercially available dielectric polymer used for energy storage, has a remarkable breakdown strength of ≈700 MV m^{-1} and ultralow loss, but can only operate continuously at temperatures up to 85 °C and for a short duration with significant derating at 105 °C.[14,15] Many heat resistant polymers have been designed and studied for high-temperature applications, but they are incapable of operating at an electric field similar to BOPP.[11,16,17] This is because their conjugated aromatic backbones that are able to withstand high temperature, built at the cost of largely reduced bandgaps, lead to high electrical conductivities and poor energy densities especially at elevated temperatures. Recent efforts for enhanced energy storage performance at high temperature via nanocomposites or coating modifications of polymer films, although encouraging, are prohibitively challenging for industrial-scale production due to requirements of (either) materials cost and (or) laborious multi-step synthesis and processing.[2,12,13,18,19] As a result, BOPP is still used today with cumbersome active cooling. The availability of flexible polymer dielectrics, capable of stable operation under ultrahigh electric field and elevated temperature is the limiting factor for high power density electrification and electronics.

Due to hot carrier excitation, injection, and transport, assisted under thermal and electric extremes, polymers exhibit a nonlinear increase in electrical conduction,[20–22] leading to the reduction of the discharged energy density, largely increased energy loss and ultimately dielectric breakdown failure[23]. While the complexity of these processes makes the study of engineering conduction mechanism under critical electric fields far from fully understood, past studies revealed the dominant role of the bandgap in determining electrical conduction and intrinsic breakdown strength of the polymer dielectrics.[20,24–27] However, careful evaluation of common high-temperature polymers reveals, unfortunately, an inverse

Dr. C. Wu, Dr. Z. Li, Dr. Y. Wang, Prof. Y. Cao
Electrical Insulation Research Center
University of Connecticut
Storrs, CT 06269, USA
E-mail: yang.cao@uconn.edu
A. A. Deshmukh, A. Alamri, Prof. G. A. Sotzing
Institute of Materials Science
University of Connecticut
Storrs, CT 06269, USA
E-mail: g.sotzing@uconn.edu
Dr. L. Chen, Prof. R. Ramprasad
School of Materials Science and Engineering
Georgia Institute of Technology
Atlanta, GA 30332, USA
The ORCID identification number(s) for the author(s) of this article can be found under https://doi.org/10.1002/adma.202000499.

DOI: 10.1002/adma.202000499

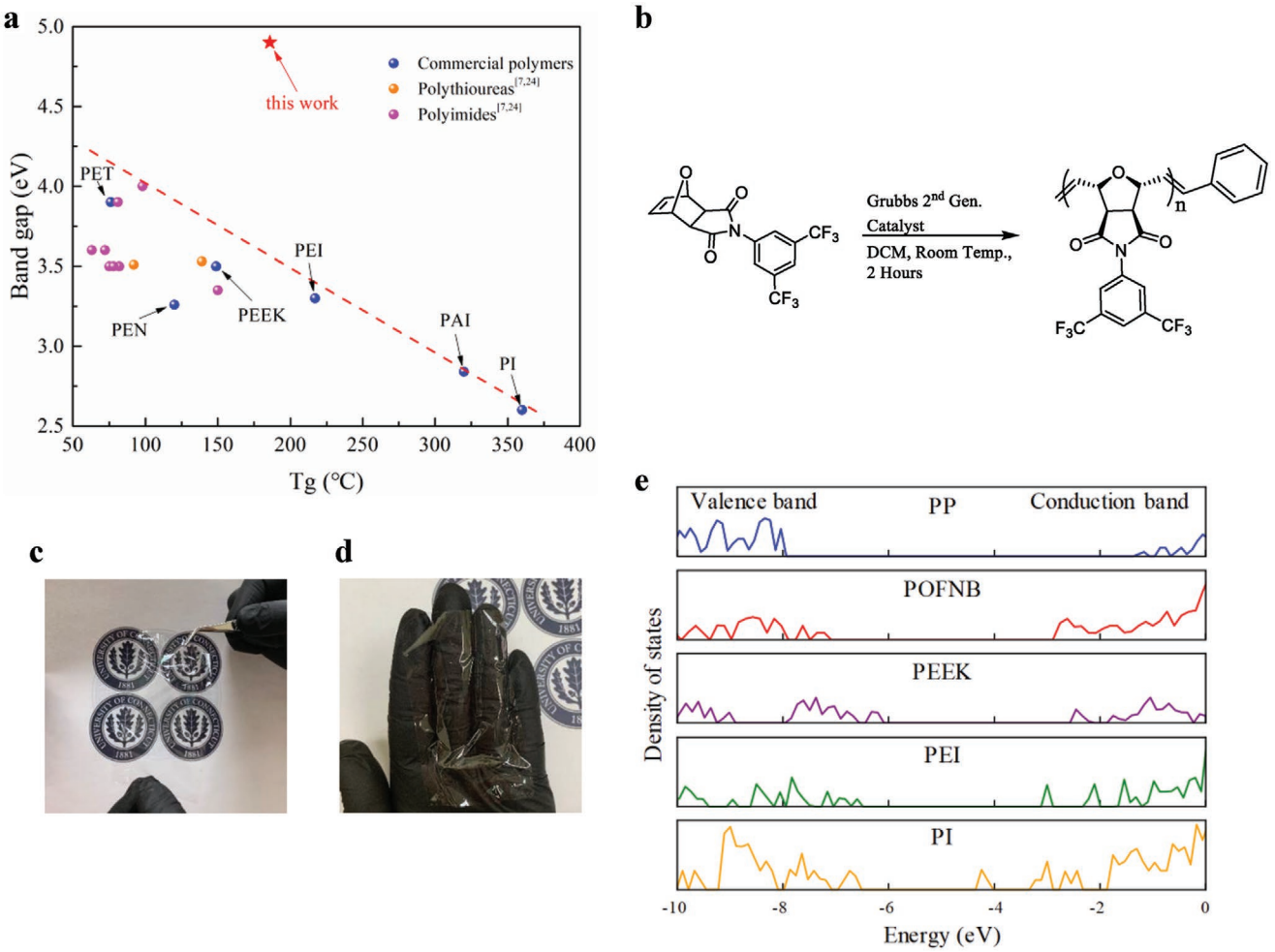

Figure 1. Material design. a) The bandgap versus. glass transition temperature for POFNB and high-temperature polymers with aromatic backbone structure (Figure S1, Supporting Information). b) Schematic of the synthesis process for POFNB. c,d) Photographs of the free-standing POFNB films. e) The electronic density of states of POFNB, PP, PEEK, PEI, and PI, computed based on density functional theory.

correlation between their bandgaps and glass transition temperatures (T_g), (**Figure 1**a, Figure S1, Supporting Information). This is because these conventional high-temperature polymers are originally engineered for high thermal stability with a backbone consisting of a large number of aromatic groups, forming conjugated planar segments that can π–π stack having diminished bandgaps. Lowering of bandgap results in inevitably compromised high field performance and poor discharged energy density, especially at high temperatures.

Here we introduce an all organic polymer, polyoxafluoronorbornene (POFNB), with saturated fused bicyclic structure in the backbone, rather than the aromatic structures, to break the aforementioned design constraint. In POFNB, the nonplanar structure avoiding π–π stacking and nonconjugated polymer backbones could restrict charge mobility between and along polymer chains concurrently. With this strategy, a large bandgap (4.9 eV, derived from UV–visible spectroscopy, see Figure S2, Supporting Information) and high glass transition temperature (186 °C) are achieved simultaneously, making POFNB an outlier compared to common high-temperature polymers, as illustrated in Figure 1a. POFNB is synthesized by a ring-opening metathesis polymerization using Grubbs generation 2 catalyst (Figure 1b, Figures S3–S9, Supporting Information) and solution cast into flexible free-standing films (Figures 1c,d).

The electronic structures of POFNB, BOPP, poly(ether ether ketone) (PEEK), polyetherimide (PEI), and polyimide (PI) were studied using density functional theory (DFT) computation (Figure S10, Supporting Information). The electronic density of states (DOS) of these polymers are illustrated in Figure 1e. Bandgaps of the investigated polymers follow the order of PP > POFNB > PEEK > PEI > PI. The bandgap from the computed DOS agrees favorably with the experimental data. The aromatic rings within PEEK, PEI, and PI contribute to high π bonding (low π^* anti-bonding) energy levels, lowering the bandgaps, while POFNB exhibits a large bandgap, the largest among the high-temperature polymers with $T_g > 100$ °C.

The high electric field energy storage performance was demonstrated using a dielectric displacement–electric field (*DE*) loop test at ambient and elevated temperatures (**Figures 2**a–c, Figures S11–S19, Supporting Information). The narrow regions inside the *DE* loops suggest the low energy dissipation of POFNB. At ambient temperature, POFNB exhibits

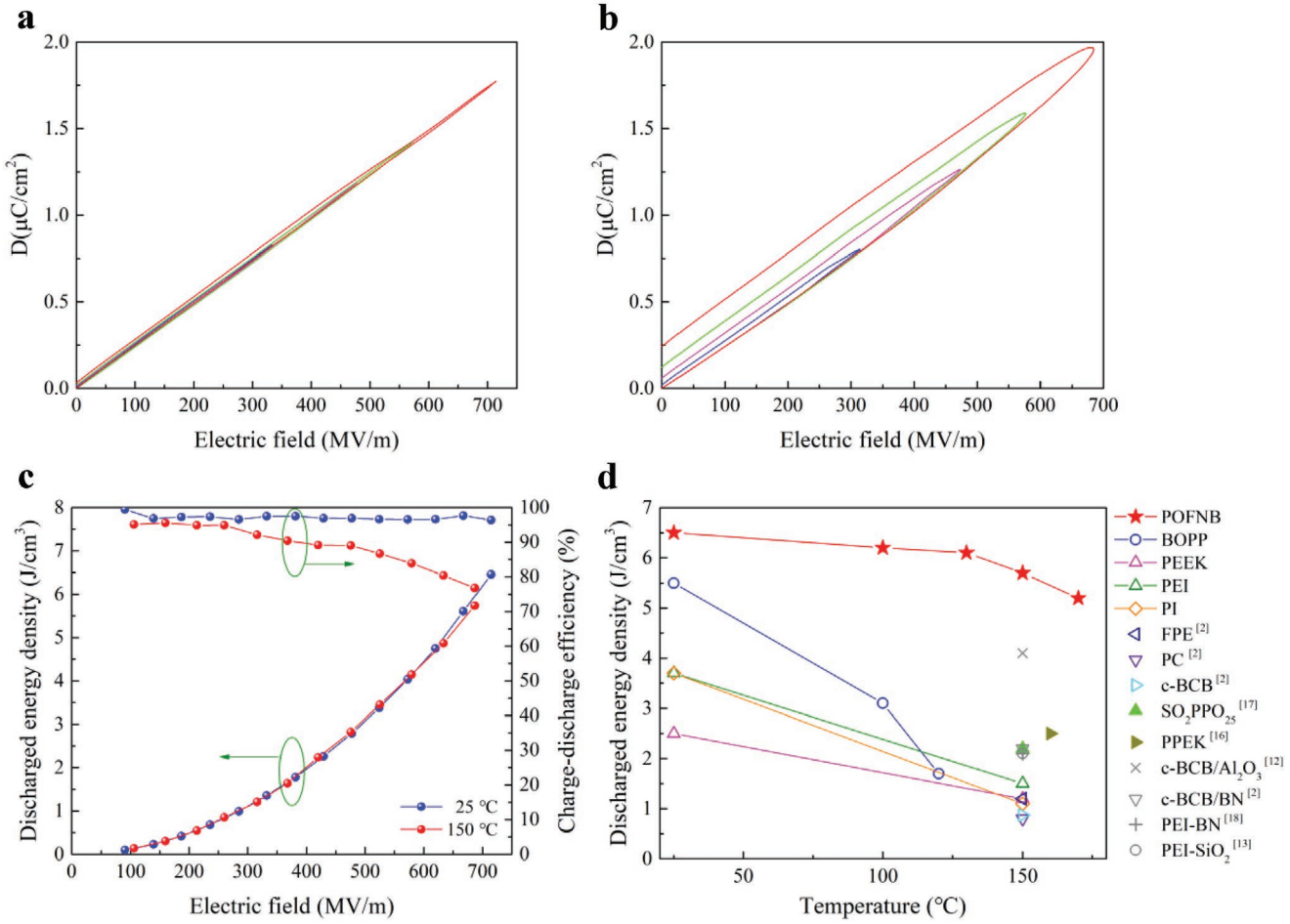

Figure 2. a,b) High electric field energy storage. Electric displacement–electric field loop (*DE* loop) of POFNB at 25 °C (a) and 150 °C (b). c) Discharged energy density and discharge efficiency of POFNB as a function of the electric field at 25 °C and 150 °C. d) Discharged energy density of POFNB at ambient and elevated temperatures relative to the best reported dielectric polymers or polymer composites. The reference polymers are poly(phthalazinone ether ketone)[16] and modified sulfonylated poly(2,6-dimethyl-1,4-phenylene oxide).[17] The reference composite systems are c-BCB (crosslinked divinyltetramethyldisiloxane-bis(benzocyclobutene) filled with aluminum oxide[12] and boron nitride (BN) nanosheet,[2] PEI films coated with BN nanosheet,[18] and silicon oxide.[13]

ultrahigh discharge efficiency (96.5%) even when the electric field exceeds 700 MV m^{-1}. At 150 °C, the discharge efficiency of POFNB at 200 MV m^{-1} (the operating electric field of commercial BOPP), is higher than 94%. Thus, an electronic system with BOPP can be readily replaced by POFNB for operation at 150 °C. More importantly, this could eliminate the cumbersome cooling system currently needed for energy storage systems with BOPP. Stable high discharged energy density is observed for POFNB over the entire temperature range investigated, far outperforming the best flexible polymer and polymer composite films reported (Figure 2d) to date.[2,12,13,16–18] In addition, at 150 °C, the energy loss of POFNB is far below that of the existing heat resistant polymers of PI, PEI, and PEEK, which exhibit high energy loss in the range of 50–70% even under relatively low electric field (Figure S19, Supporting Information).

Fundamentally the capacitive energy storage originates from the dielectric polarization. The strategy for the design of a polymer having a stable dielectric constant and low polarization loss over a broad temperature range would require that all rigid segments having restricted rotation remain restricted while all freely rotatable single bonds continue to freely rotate across the entire temperature range for operation.[28,29] As such, close attention needs to be paid to elements that can be involved in conjugation. For example, an element that could result in partial double bond in conjugation with a sp^2 hybridized carbon could become freely rotating at a higher temperature, contributing to a temperature dependent polarization. To gain more insight into its highly stable discharged energy density, the dielectric constant of POFNB was investigated in a wide frequency and temperature range (**Figure 3**a). The dielectric constant of POFNB stays remarkably stable at around 2.5 with a low dissipation factor of <0.5%. Even down to –160 °C, the dielectric constant holds stable (Figure S20, Supporting Information). The temperature coefficient of dielectric constant for POFNB is 0.016% $°C^{-1}$, the least among commonly known polymers such as BOPP (0.061% $°C^{-1}$), PEEK (0.085% $°C^{-1}$), PEI (0.022% $°C^{-1}$), and PI (0.042% $°C^{-1}$) (Figure 3b, Figures S21–S24, Supporting Information). Importantly, with the molecular design of POFNB, the imide ring is fused to the backbone five-membered ring allowing for an elongated rigid bicyclic structure extending

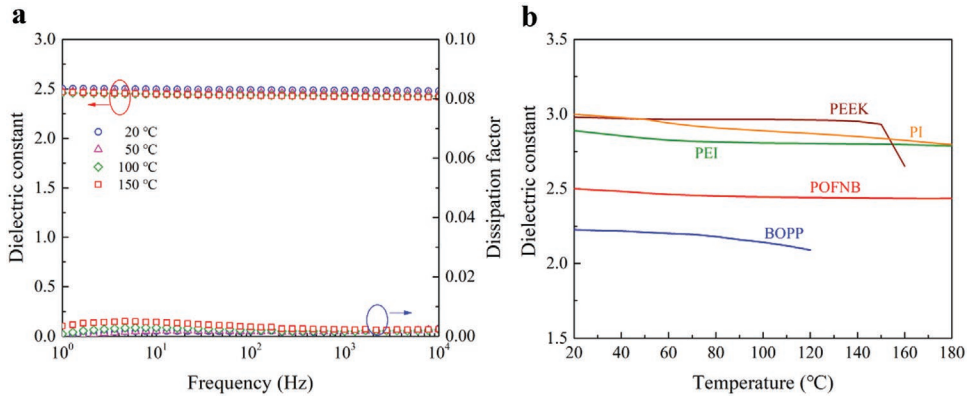

Figure 3. Dielectric polarization and loss. a) Dielectric constant and dissipation factor of POFNB at ambient and elevated temperatures. b) Temperature dependence of dielectric constant at 1000 Hz for POFNB, BOPP, PEEK, PEI, and PI.

from the backbone analogous to a piston rod of a crankshaft. The imide functionality further provides a connection to the benzene ring such that the nitrogen has insignificant conjugation with the sp^2 carbon of the benzene ring since it is tied up in cross conjugation with both carbonyls. Therefore, here the new design strategy imparts flexible POFNB with temperature-invariant polarization from −160 to 160 °C. Such a stable dielectric constant and low dissipation factor over a wide temperature and frequency range are highly preferred capacitive characteristics to ensure a highly stable and superior system performance.[11]

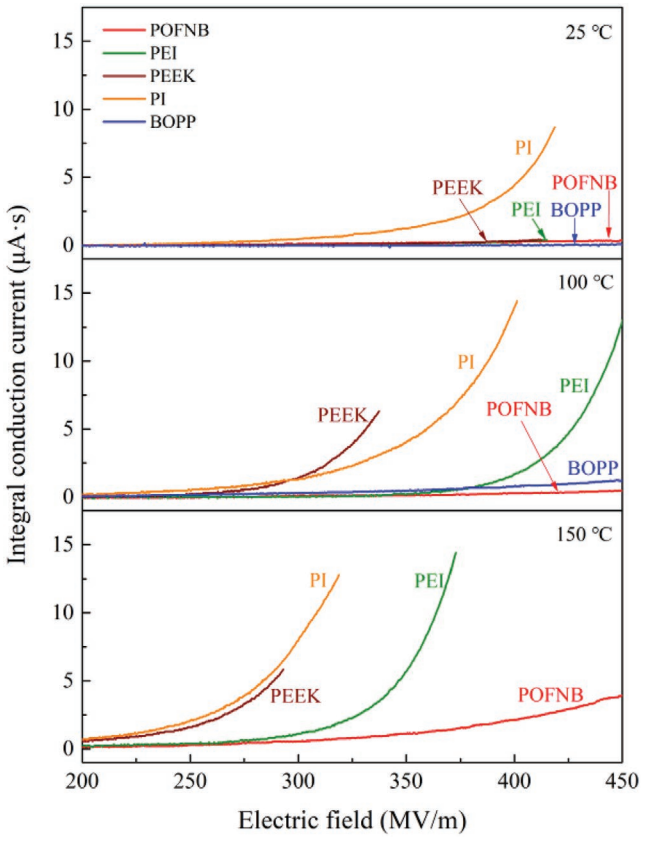

Figure 4. Conduction as a function of the electric field. Integral conduction current investigated by a designed transient measurement system for POFNB, BOPP, PEEK, PEI, and PI. Conduction current densities as a function of the electric field are illustrated in Figures S25–S27, Supporting Information obtained from the derivative of the time integral current.

In addition to the polarization loss, conduction loss dominates at high electric field due to strong electric field and temperature-dependent charge injection and transport.[13,20,30] With a specially designed system, pre-breakdown conduction in polymer dielectrics can be measured with high precision via dynamic cancellation of the capacitive current so as to small resistive conductions down to 10 ppm level can be probed during voltage ramp[31] (**Figure 4**, Figures S25–S27, Supporting Information). As shown in Figure 4, at room temperature, POFNB reveals highly suppressed conduction current under high electric field and more pronounced suppression at elevated temperatures. At temperatures over 100 °C, POFNB exhibits much lower conduction than BOPP and all other high-temperature polymers. The electrical conduction for POFNB at 150 °C is almost two orders of magnitude lower in a side-by-side comparison with the best commercial high-temperature dielectric polymer films (Figure S27, Supporting Information) and the best reported ceramic films[4]. The hopping conduction model was utilized to reveal the contribution of large bandgap of POFNB to the suppression on conduction current (Figure S28, Supporting Information). Building upon the large bandgap, charges could not move over the energy barrier between adjacent sites in the form of hopping for POFNB. In contrast to POFNB whose conduction stays always low even at 150 °C, PI, PEI, and PEEK all exhibit strong charge injection/conduction, particularly at temperatures >100 °C, indicating once again the fundamental limit associated with these conventional high-temperature polymers designed with conjugated aromatic backbones. Even though PEI and PEEK also exhibit low conduction current at room temperature, the sharp increase of conduction current at elevated temperature suggests that charges with increased thermally assisted excitation energy can overcome the energy barrier between the localized sites. With the lowest bandgap, PI exhibits intense conduction towards high electric field even at room temperature. Additionally, suppression on conduction current inhibits the heat runaway induced degradation and hence breakdown, ensuring the reliability of the dielectric film in harsh environments.[20,30]

In summary, an all-organic dielectric polymer POFNB is proposed for capacitive energy storage at elevated temperatures. The uniqueness of POFNB with fused bicyclic olefin and alkenes separated by freely rotating single bonds as backbones, polar aromatic structure extending from the backbone analogous to a piston-like crankshaft, endowing it with large bandgap and flexibility. Built upon its large bandgap and high T_g, POFNB offers intrinsically stable and temperature invariant high electric field dielectric characteristics, especially at elevated temperatures. Free from crosslinking or any other additional processing, POFNB can be readily processed into a free-standing film by a roll-to-roll process. The facile processability and flexibility ensure its scalability for flexible electronic devices. Coupled with the versatile ring-opening metathesis polymerization (ROMP) synthesis, POFNB provides sufficient material design and synthesis space for further performance optimization.

Experimental Section

Materials: Exo-3,6-epoxy-1,2,3,6-tetrahydrophthalic anhydride (Oxanorbornene anhydride), anhydrous toluene, ethyl ether, dichloromethane (DCM), tetrahydrofuran (THF), methanol, and acetic anhydride were purchased from Fisher Scientific. Anhydrous sodium acetate and 3,5-bis(trifluoromethyl)aniline were purchased from Oakwood Chemicals. Grubbs generation 2 catalyst was purchased from Sigma-Aldrich. The synthesis details can be found in the Supporting Information.

Characterizations: ^{1}H NMR analysis was studied with Bruker AVANCE 500 MHz spectrometer using TMS as an internal standard. Fourier-transform infrared spectroscopy (FTIR) was done using a KBr pellet method with Nicolet Magna 560 IR spectrometer. Differential scanning calorimetry was performed using a TA Instruments DSC Q-100 differential scanning calorimeter. Thermogravimetric analysis was performed using a TA Instruments TGA Q-500 at a heating rate of 20 °C min^{-1}. The molecular weight of POFNB was determined using a Waters GPC system with dimethylacetamide as a mobile phase and PMMA as a standard.

DFT Calculation: Physical and electronic structures of polymers have been investigated using first-principles density functional theory (DFT), implemented in the Vienna Ab initio Simulation Package (VASP). In the calculations, crystal slabs of PP and PEEK were modeled while oligomers with six repeat units were used for amorphous polymers (i.e., POFNB, PEI, and PI). To fully relax these structures, the Perdew–Burke–Ernzerhof exchange–correlation functional, a plane-wave energy cutoff of 400 eV, and the vdW- DF2 functional were used. The adopted Monkhorst–Pack k-point meshes of $4 \times 1 \times 4$, $1 \times 5 \times 1$, and $1 \times 1 \times 1$ were used for PP, PEEK, and other polymers (i.e., POFNB, PEI, and PI), respectively. The obtained structures were further used to study the electronic structure using the Heyd–Scuseria–Ernzerhof HSE06 functional.

High Field Displacement–Electric Field Loop Measurement: Displacement–electric field loop was employed using a modified Sawyer–Tower polarization loop tester with a unipolar positive half sinusoidal wave of 100 Hz. The measurement system consisted of a Trek Model 10/40 10 kV high voltage amplifier and an OPA541 operational amplifier-based current-to-voltage converter. Gold/palladium electrodes are coated on both sides of the film with a diameter of 3 mm using the sputter coating method to ensure a good contact between electrodes and the film.

Dielectric Spectroscopy: The measurement was conducted using a Solartron SI 1260 frequency response analyzer with a Solartron 1296 dielectric interface. The sample in a test cell was put in an oven with a Delta Design 9015 temperature controller, which can control the temperature fluctuation within ±0.5 °C in the whole measurement. The measurement was carried out at temperature starting from 20 °C with an increasing step of 10 °C. Before each measurement, a 30 min stabilization at a set temperature was used to guarantee the sample was in a uniform steady isothermal state. The temperature coefficient C_T of the dielectric constant is obtained via Equation (1), where ε_{ri} is dielectric constant at temperature T_i and T_0 is 20 °C.

$$C_T = \left|\frac{\Delta \varepsilon_r}{\Delta T}\right| \times 100\% = \left|\frac{\varepsilon_{ri} - \varepsilon_{r0}}{T_i - T_0}\right| \times 100\% \quad (1)$$

High Electric Field Conduction: The conduction at the high field was measured with a specially designed measurement system which can dynamically cancel the capacitive component of the current.[31] The system uses a small sinusoidal modulation signal superimposed on the voltage ramp to track the capacitive current under transient condition. Using the negative feedback loop formed with a dual-phase lock-in amplifier, the capacitive current can be actively canceled via dynamic gain control throughout the measurement. The remaining signal output represents the time-integrated conduction current across the sample, with accuracy for the small resistive current down to 10 ppm.

Supporting Information

Supporting Information is available from the Wiley Online Library or from the author.

Acknowledgements

C.W. and A.A.D. contributed equally to this work. This work is supported through a multidisciplinary university research initiative (MURI) grant (N00014-17-1-2656) and a capacitor program grant (N0014-19-1-2340), both from ONR. The authors would like to thank Michael Sotzing and JoAnne Ronzello for their assistance in dielectric spectra measurement. They thank Prof. Mukerrem Cakmak and Zeynep Mutlu from Materials and Mechanical Engineering of Purdue University for the wide-angle X-ray scattering (WAXS) measurements.

Conflict of Interest

The authors declare no conflict of interest.

Keywords

capacitors, elevated temperature, energy storage, large bandgap, polymer dielectrics

Received: January 21, 2020
Revised: February 25, 2020
Published online:

[1] W. J. Sarjeant, J. Zirnheld, F. W. MacDougall, *IEEE Trans. Plasma Sci.* **1998**, *26*, 1368.
[2] Q. Li, L. Chen, M. R. Gadinski, S. Zhang, G. Zhang, H. U. Li, E. Iagodkine, A. Haque, L. Chen, T. N. Jackson, Q. Wang, *Nature* **2015**, *523*, 576.
[3] B. Chu, X. Zhou, K. Ren, B. Neese, M. Lin, Q. Wang, F. Bauer, Q. M. Zhang, *Science* **2006**, *313*, 334.
[4] H. Pan, F. Li, Y. Liu, Q. Zhang, M. Wang, S. Lan, Y. Zheng, J. Ma, L. Gu, Y. Shen, P. Yu, S. Zhang, L. Chen, Y. Lin, C. Nan, *Science* **2019**, *365*, 578.

[5] J. Jiang, Z. Shen, X. Cai, J. Qian, Z. Dan, Y. Lin, B. Liu, C. W. Nan, L. Chen, Y. Shen, *Adv. Energy Mater.* **2019**, *9*, 1803411.
[6] Y. Wang, J. Cui, Q. Yuan, Y. Niu, Y. Bai, H. Wang, *Adv. Mater.* **2015**, *27*, 6658.
[7] A. Mannodi-Kanakkithodi, G. M. Treich, T. D. Huan, R. Ma, M. Tefferi, Y. Cao, G. A. Sotzing, R. Ramprasad, *Adv. Mater.* **2016**, *28*, 6277.
[8] J. Watson, G. Castro, *J. Mater. Sci.: Mater. Electron.* **2015**, *26*, 9226.
[9] K. C. Reinhardt, M. A. Marciniak, *Proc. Energy Conversion Engineering Conf.*, IEEE, Washington, DC, USA **1996**,p. 127.
[10] C. Buttay, D. Planson, B. Allard, D. Bergogne, P. Bevilacqua, C. Joubert, M. Lazar, C. Martin, H. Morel, D. Tournier, C. Raynaud, *Matter. Sci. Eng.: B* **2011**, *176*, 283.
[11] J. S. Ho, S. G. Greenbaum, *ACS. Appl. Mater. Inter.* **2018**, *10*, 29189.
[12] H. Li, D. Ai, L. Ren, B. Yao, Z. Han, Z. Shen, J. Wang, L. Q. Chen, Q. Wang, *Adv. Mater.* **2019**, *31*, 1900875.
[13] Y. Zhou, Q. Li, B. Dang, Y. Yang, T. Shao, H. Li, J. Hu, R. Zeng, J. He, Q. Wang, *Adv. Mater.* **2018**, *30*, 1805672.
[14] D. Tan, L. Zhang, Q. Chen, P. Irwin, *J. Electron. Mater.* **2014**, *43*, 4569.
[15] M. Rabuffi, G. Picci, *IEEE Trans. Plasma Sci.* **2012**, *30*, 1939.
[16] J. Pan, K. Li, S. Chuayprakong, T. Hsu, Q. Wang, *Appl. Mater. Inter.* **2010**, *2*, 1286.
[17] Z. Zhang, D. H. Wang, M. H. Litt, L. Tan, L. Zhu, *Angew. Chem.* **2018**, *130*, 1544.
[18] A. Azizi, M. R. Gadinski, Q. Li, M. A. AlSaud, J. Wang, Y. Wang, B. Wang, F. Liu, L. Chen, N. Alem, Q. Wang, *Adv. Mater.* **2017**, *29*, 1701864.
[19] Q. Li, F. Liu, T. Yang, M. R. Gadinski, G. Zhang, L. Chen, Q. Wang, *Proc. Nat. Acad. Sci. USA* **2016**, *113*, 9995.
[20] L. A. Dissado, J. C. Fothergill, *Electrical Degradation and Breakdown in Polymers*, IET, London, UK **1992**.
[21] M. Ieda, *IEEE Trans. Electr. Insul.* **1984**, *EI-19*, 162.
[22] J. Ho, T. R. Jow, *IEEE Trans. Dielectr. Electr. Insul.* **2012**, *19*, 990.
[23] Z. Shen, J. Wang, J. Jiang, S. X. Huang, Y. Lin, C. Nan, L. Chen, Y. Shen, *Nat. Commun.* **2019**, *10*, 1843.
[24] V. Sharma, C. Wang, R. G. Lorenzini, R. Ma, Q. Zhu, D. W. Sinkovits, G. Pilania, A. R. Oganov, S. Kumar, G. A. Sotzing, S. A. Boggs, R. Ramprasad, *Nat. Commun.* **2014**, *5*, 4845.
[25] Y. Sun, S. A. Boggs, R. Ramprasad, *Appl. Phys. Lett.* **2012**, *101*, 132906.
[26] L. Chen, T. D. Huan, Y. C. Quintero, R. Ramprasad, *J. Mater. Sci.* **2016**, *51*, 506.
[27] L. Chen, R. Batra, R. Ranganathan, G. Sotzing, Y. Cao, R. Ramprasad, *Chem. Mater.* **2018**, *30*, 7699.
[28] C. Wu, Z. Li, G. M. Treich, M. Tefferi, R. Casalini, R. Ramprasad, G. A. Sotzing, Y. Cao, *Appl. Phys. Lett.* **2019**, *115*, 163901.
[29] Z. Li, G. M. Treich, M. Tefferi, C. Wu, S. Nasreen, S. K. Scheirey, R. Ramprasad, G. A. Sotzing, Y. Cao, *J. Mater. Chem. A* **2019**, *7*, 15026.
[30] M. Ieda, M. Nagao, M. Hikita, *IEEE Trans. Dielectr. Electr. Insul.* **1994**, *1*, 934.
[31] Z. Li, C. Xu, H. Uehara, S. Boggs, Y. Cao, *AIP Adv.* **2016**, *6*, 115025.